Available online at www.sciencedirect.com
ScienceDirect
Polymer 48 (2007) 1219–1228
polymer
www.elsevier.com/locate/polymer

In situ ATR-FT-IR study of the thermal decomposition of diethyl peroxydicarbonate in supercritical carbon dioxide

William Z. Xu, Xinsheng Li, Paul A. Charpentier*

Faculty of Engineering, Department of Chemical and Biochemical Engineering, University of Western Ontario, TEB 437, London, Ontario, Canada N6A 5B9

Received 7 June 2006; received in revised form 10 November 2006; accepted 12 December 2006
Available online 17 December 2006

Abstract

The thermal decomposition of the organic free-radical initiator, diethyl peroxydicarbonate (DEPDC), was monitored by *in situ* ATR-FT-IR in heptane, and in the green solvent supercritical carbon dioxide ($scCO_2$) both with and without supercritical ethylene. It was observed that the characteristic peaks of DEPDC at 1802–1803 and 1194–1203 cm^{-1} decreased significantly upon heating corresponding to the decomposition of DEPDC, while two new intense peaks simultaneously appeared at 1747 and 1262 cm^{-1} in heptane, and similarly at 1756 and 1250 cm^{-1} in $scCO_2$. The changes in the absorbance intensity of the characteristic peaks of the initiator during the decomposition were used for the measurement of the decomposition rate constant (k_d) of DEPDC. It was found that the thermal decomposition of DEPDC at low concentration in either heptane under atmospheric N_2 or $scCO_2$ under high pressure was via the first-order kinetics of unimolecular decomposition. The activation energy of the thermal decomposition of DEPDC was found to be 115 kJ/mol in heptane from 40 to 74 °C and 118 kJ/mol in $scCO_2$ from 40 to 60 °C. These new peaks revealed the formation of carboxyl groups contained in the decomposed products, indicating incomplete decarboxylation. During removal of CO_2 after the reaction in $scCO_2$, the instable intermediate monoethyl carbonate was decarboxylated and converted into the major end product, ethanol.

Keywords: ATR-FT-IR; Initiator; Kinetics and mechanism

1. Introduction

Considerable effort has been devoted in recent years to find environmentally benign solvents and processes, particularly as a result of increased environmental regulations concerning the use of volatile organic compounds (VOCs) [1–6]. Supercritical carbon dioxide ($scCO_2$) has emerged as a viable ''green'' alternative to organic solvents for several applications, including polymer synthesis, modification, and nanotechnology [7,8]. In the supercritical state ($T_c = 31.8$ °C, $P_c = 76$ bar), carbon dioxide can have unique properties such as liquid-like density and gas-like diffusivity, and these properties are ''tunable'' by varying the pressure and/or temperature [9]. Previously, DeSimone and coworkers have shown that $scCO_2$ is a promising alternative medium for free radical, cationic, and step-growth polymerizations [1,3,10]. Indeed, DuPont has recently commissioned a plant to manufacture Teflon™ in $scCO_2$ by the use of free-radical polymerization [11]. The reasons for the intense industrial interest are that CO_2 is inert to highly electrophilic radicals (i.e., no chain transfer to solvent), inexpensive, non-toxic, non-flammable, and environmentally benign [3].

In recent years, considerable attention has been attracted to investigate and study the mechanism of free-radical formation and the kinetics of the decomposition of organic peroxides [12–21], particularly due to their applications in organic synthesis [12,13], biological processes [14,15], polymerization [16,17], and as resin modifiers [18], additives for fuel [19], and explosives [20]. Free radical polymerization still dominates in the production of many commercial polymers such as polystyrene, polyethylene (low density), poly(ethylene-co-vinyl acetate), Teflon, and other fluorinated polymers. Due to the proven ability of $scCO_2$ in industrial continuous polymerizations, and a poor understanding of how CO_2

* Corresponding author. Tel.: +1 519 661 3466; fax: +1 519 661 3498.
E-mail address: pcharpentier@eng.uwo.ca (P.A. Charpentier).

0032-3861/$ - see front matter © 2006 Elsevier Ltd. All rights reserved.
doi:10.1016/j.polymer.2006.12.018

influences reaction kinetics, a study of the chemistry of the thermal decomposition of the required organic peroxide initiators under supercritical conditions is important to understand and control the polymerizations under these conditions.

Dialkyl peroxydicarbonates $(R-O-CO_2)_2$ are used as free-radical initiators in many commercial processes such as the large-scale production of polymers and curing resins [12,18,21]. Compared with other classes of peroxides, the number of mechanistic studies on the decomposition of dialkyl peroxydicarbonates is relatively small, particularly in green solvents. According to the previous studies [16,22–26], a general decomposition mechanism of peroxydicarbonates or peroxyesters can be described as direct decomposition of the peroxides through breaking the weak O–O bond. The resulting alkoxycarboxyl or carbonyloxy radical may either decarboxylate [24–28] or participate in a bimolecular reaction [22,23]. In addition, solvents may have some influence on the decomposition of peroxydicarbonates as the employed solvent is seldom inert due to the high activity of the formed free radicals. Thermal decomposition of initiators in supercritical CO_2 has been studied by Guan *et al*. [29], Bunyard [30], Charpentier *et al*. [4,5,31] and Kadla *et al*. [32]. It was reported that the rate constants of initiator decomposition in $scCO_2$ were different from that in other organic solvents due to its ''zero-viscosity'' [30] and low dielectric constant [29]. Charpentier *et al*. studied the thermal decomposition of diethyl peroxydicarbonate (DEPDC) in $scCO_2$ in a continuous stirred tank reactor (CSTR) [31], wherein reaction kinetics were simulated based on a one-bond radical fission mechanism. However, this study did not harness the power of *in situ* ATR-FT-IR.

Hence, the goal of the present work was to study the decomposition of a previously studied initiator DEPDC in high-pressure $scCO_2$ and ethylene using high pressure *in situ* ATR-FT-IR, and to compare the kinetic decomposition results with previous non-FT-IR techniques. Offline NMR was used as a complementary tool for studying the decomposition mechanism. Understanding the initiator decomposition by ATR-FT-IR in $scCO_2$ is the first step for analyzing more complex spectroscopic data during polymerizations to provide an understanding of the formation of inorganic/organic hybrids for our work in the one-pot synthesis of polymer nanocomposites.

2. Experimental

2.1. Materials

Ethylene (99.99% Polymer Grade) was purchased from Matheson Gas Products Canada, and further passed through columns filled with 5 Å molecular sieves and reduced 20% copper oxide/Al_2O_3 to remove moisture and oxygen, respectively. Instrument grade CO_2 (from BOC Gases, 99.99%, with dip-tube) was purified by passing through columns filled with 5 Å molecular sieves and reduced 20% copper oxide/Al_2O_3 to remove moisture and oxygen, respectively. Ultra high-purity N_2 (from BOC, 99.99%) was further purified by passing through columns filled with 5 Å molecular sieves and reduced 20% copper oxide/Al_2O_3 to remove moisture and oxygen, respectively. The initiator diethyl peroxydicarbonate (DEPDC) was homemade as described below. Heptane (Aldrich, HPLC grade) was distilled under vacuum. NaOH, 30% H_2O_2, ethyl chloroformate, 0.1 N sodium thiosulfate solution, sodium bicarbonate, sodium sulfate, glacial acetic acid, potassium iodide, and diethyl carbonate were purchased from Aldrich and used as received.

2.2. Preparation of DEPDC initiator

Distilled water (100 ml) was charged in a glass reactor (250 ml) equipped with a magnetic agitator and a thermometer. The reactor was cooled to ≤ 5 °C in an ice/water bath. Ethyl chloroformate (12 ml) and 30% H_2O_2 (6.64 g) were added to the reactor under powerful stirring. Then NaOH solution (24 ml, 5 N) was introduced to the reactor dropwise. The reaction was carried out under gentle stirring for 10 min with the reaction temperature controlled below 10 °C. Heptane was utilized to extract the formed DEPDC from the mixture and the solution was dried over sodium sulfate. The dried solution was filtered and separated from the solvent by means of a rotary evaporator under vacuum at less than 2 °C. The yield of DEPDC was measured using a standard iodimetric titration analysis technique (ASTM E298-91) to exceed 90%. *Owing to the instability of DEPDC, highly concentrated DEPDC must be stored at very low temperature (−20 °C). Scheme 1 provides the overall reaction.

2.3. Reactor and in situ ATR-FT-IR measurements

In situ Fourier transform infrared (FT-IR) monitoring of solution concentration in the stirred 100 ml high-pressure autoclave (Parr 4842) was performed using a high-pressure immersion probe (Sentinel-Mettler Toledo AutoChem). The DiComp ATR probe consists of a diamond wafer, a gold seal, a ZnSe support/focusing element, housed in alloy C-276. The probe was attached to an FT-IR spectrometer (Mettler Toledo AutoChem ReactIR 4000) via a mirrored optical conduit, connected to a computer, supported by ReactIR 2.21 software (MTAC). This system uses a 24-hour HgCdTe (MCT) photoconductive detector. The light source is a glow bar from which the interferometer analyzes the spectral region from 650 to 4000 cm^{-1}. The beamsplitter inside the RIR4000 is ZnSe. Spectra were recorded at a resolution of 2 cm^{-1} and the absorption spectra were the results of 64 scans. *In situ* ATR-FT-IR was applied to monitor the thermal decomposition of DEPDC and the product formation.

2.4. Gas chromatography–mass spectrometry

Gas chromatography–mass spectrometry (GC–MS) (Varian, Saturn 2100D/GC–MS) was applied to analyze the

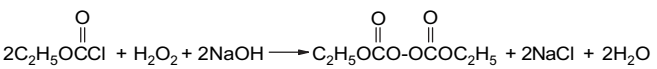

Scheme 1. The overall reaction of synthesis of DEPDC.

decomposed products of DEPDC with the injector being used as a microreactor to study the DEPDC decomposition behavior. The injector temperature was controlled from its minimum temperature 50 to 200 °C. The column temperature was controlled by programming segments, 30 °C for 20 min, then increased to 50 °C at 10 °C/min, and kept at this temperature for 20 min, then increased to 100 °C at 10 °C/min, and kept at this temperature for 40 min with the purpose of analyzing the high carbon number compounds as well as purging the column for the next sample measurement. The mass spectrum was fitted with the standard spectra from the Varian library.

2.5. Nuclear magnetic resonance

Nuclear magnetic resonance (NMR) spectra were recorded using a Varian Inova 600 or 400. ^{1}H and ^{13}C NMR chemical shifts are reported relative to TMS. Proton − 400.087 MHz, PW90 (90 pulse width) = 12.3 μs (PW45 used in 1D experiment), number of transients (NT) = 8, acquisition time (AT) = 4.00 s, delay time (D1) = 1. Carbon − 100.613 MHz, PW90 = 10.4 μs (PW 45 used in 1D), NT = 256, AT = 1.20 s, D1 = 1. gCOSY − NT = 1, number of increment (NI for 2D) = 128 (linear prediction was used to give a final data set of 384 for processing), AT = 0.20 s, D1 = 1. gHSQC − NT = 4, NI = 128 (linear prediction used to 384 for processing), AT = 0.21 s, garp ^{13}C decoupling used, D1 = 1.

3. Results and discussion

3.1. Assignment of characteristic peaks of DEPDC

In order to provide accurate data for FT-IR interpretation, highly concentrated DEPDC initiator was synthesized without solvent (*explosive). By using a standard iodimetric titration analysis technique, the concentration of the homemade DEPDC in this study was found to be greater than 97%. The two strongest absorbance peaks of DEPDC are located at 1191 and 1794 cm^{-1}(Fig. 1a). The peak at 1191 cm^{-1} can be assigned to the C−O stretching vibration in the −C(O)−O− group, while the peak appearing at 1794 cm^{-1} is ascribed to the characteristic C═O stretching vibration in the −C(O)−O−O−C(O)− group [33,34].

3.2. Thermal decomposition of DEPDC in heptane and supercritical CO_2

In order to distinguish the characteristic peaks of DEPDC for decomposition in heptane (and later $scCO_2$), the FT-IR spectra of heptane and DEPDC/heptane were collected as shown in Fig. 1b and c. The spectrum of heptane gives absorbance peaks at 1378, 1467, 2854, 2874, 2922, and 2958 cm^{-1}. The bands appearing at 2854, 2874, 2922, and 2958 cm^{-1} are assigned to CH_2 sym., CH_3 sym., CH_2 asym., and CH_3 asym. stretching vibrations, respectively while the peaks at 1378, 1467 cm^{-1} are assigned to CH_3 sym. bending and CH_3 asym. bending/CH_2 scissoring vibrations, respectively. [33] In the solution of DEPDC/heptane, DEPDC showed strong

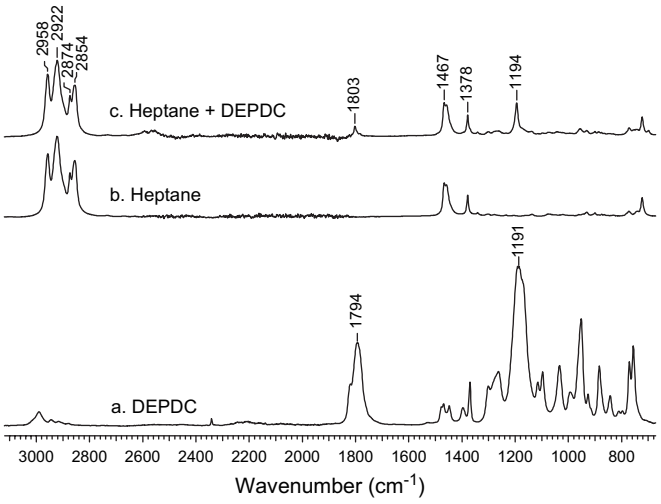

Fig. 1. IR spectra of (a) DEPDC, (b) heptane, and (c) heptane + DEPDC. Spectra were collected at ambient temperature under atmospheric pressure.

absorbance peaks at 1194 and 1803 cm^{-1} which slightly differ from the characteristic peaks of pure DEPDC at 1191 and 1794 cm^{-1}. When the DEPDC/heptane solution was heated, the thermal decomposition of DEPDC with time was monitored and clearly observed by the decrease in peak heights at 1194 and 1803 cm^{-1} (Fig. 2a–c). In order to clearly demonstrate the formation of decomposed products and the conversion of DEPDC, a further treatment was made by means of subtracting the spectrum measured before the reaction from the spectrum measured after the reaction (Fig. 2d). The appearance of the positive peaks at 1262 and 1747 cm^{-1} in the subtraction spectrum are ascribed to the formation of decomposed products.

The thermal decomposition of DEPDC in supercritical CO_2 was studied as presented in Fig. 3, which shows the spectra before and after the reaction as well as the subtraction spectrum under supercritical conditions. The characteristic peaks of DEPDC in $scCO_2$ at 1803 and 1203 cm^{-1} are clearly observed in Fig. 3a, which decreased following heating time, while new

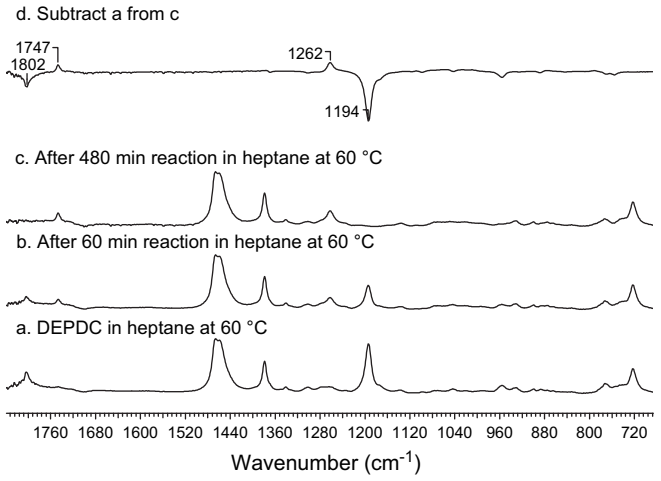

Fig. 2. *In situ* FT-IR spectra of DEPDC thermal decomposition in heptane (DEPDC concentration 2.7 wt%) at 60 °C. (a) At $t = 0$ min; (b) at $t = 60$ min; (c) at $t = 480$ min; (d) resulting spectrum from c − a subtraction.

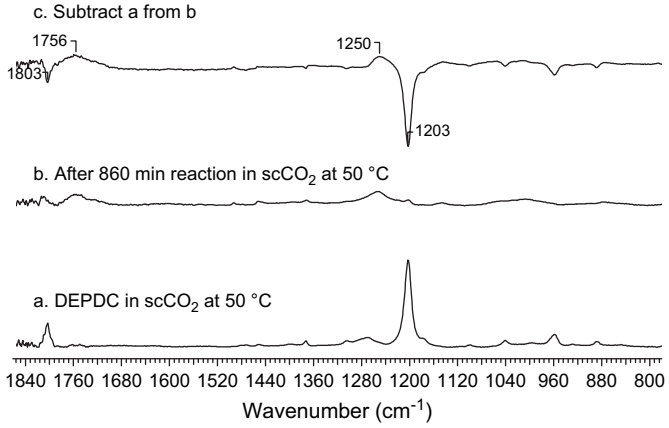

Fig. 3. *In situ* FT-IR spectra of DEPDC thermal decomposition in $scCO_2$ (DEPDC concentration 3.4 wt%) at $T = 50$ °C, 20 Mpa. (a) At $t = 0$ min; (b) at $t = 860$ min; (c) resulting spectrum from b − a subtraction.

peaks at 1756 and 1250 cm^{-1} gradually developed. The thermal decomposition of DEPDC was also studied in supercritical ethylene and supercritical ethylene/CO_2, due to our interest in the polymerization of ethylene and the synthesis of polyethylene nanocomposites in $scCO_2$, and to examine whether or not radical induced decomposition was significant. Fig. 4 displays the result of FT-IR spectra of the DEPDC/heptane before introducing ethylene and after the ethylene polymerization at 60 °C. The subtraction result (Fig. 4b − 4a) is given in Fig. 4c. Similar to that found with heptane and $scCO_2$, the conversion of DEPDC gives rise to negative peaks at 1193 and 1803 cm^{-1}, while the new species formed from decomposition of the initiator give positive peaks at 1261 and 1747 cm^{-1}. Fig. 5 plots the four peaks observed during DEPDC decomposition in $scCO_2$, with two peaks decreasing from initiator decomposition and the other two peaks increasing from product formation. The

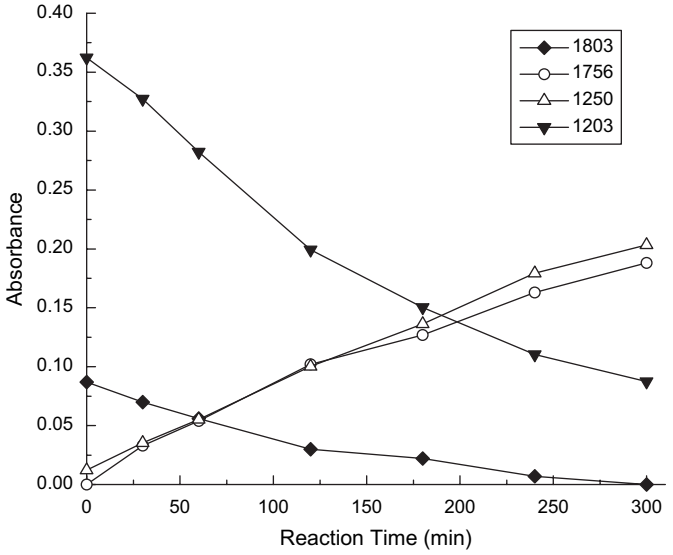

Fig. 5. *In situ* FT-IR results for absorbance versus reaction time curves for DEPDC decomposition in $scCO_2$ ($T = 60$ °C, $P = 20$ MPa, DEPDC concentration 8.8 wt%).

intensities of characteristic peaks of DEPDC were used for kinetic analysis as discussed below.

3.3. Kinetic measurement

One of the advantages of using *in situ* FT-IR for measuring initiator decomposition is that it provides direct measurement of the change in concentration of the reaction ingredients and products. The absorbance intensity is directly proportional to the concentration according to the Beer–Lambert law:

$$A = \varepsilon C l \tag{1}$$

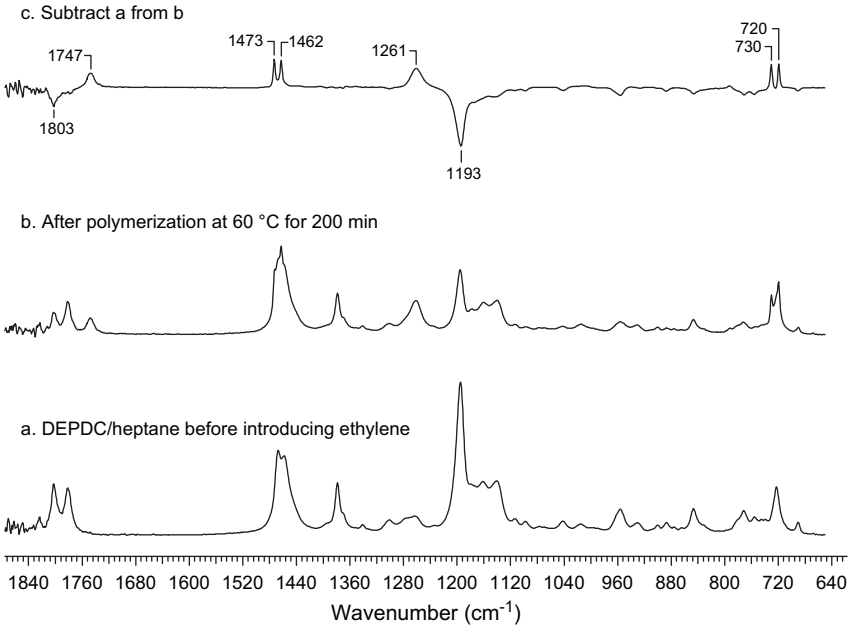

Fig. 4. *In situ* FT-IR spectra of DEPDC thermal decomposition in supercritical ethylene ($T = 60$ °C, $P = 13.8$ MPa). (a) At $t = 0$ min; (b) at $t = 200$ min; (c) resulting spectrum from b − a subtraction.

where A is the absorbance, ε is the molar absorptivity ($l\,mol^{-1}\,cm^{-1}$), C is the concentration of the compound in solution ($mol\,l^{-1}$), and l is the path length of the sample (cm). In order to examine the linear relationship between the absorbance intensity and the concentration, the FT-IR spectra of different concentrations of DEPDC in heptane at 20 °C were measured. Due to the instability of DEPDC at high temperature, diethyl carbonate was used as an alternative analog to DEPDC for examining the linear relationship in $scCO_2$ (the peak at 1269 cm^{-1} was used). An excellent linear relationship was found in both studied solvents (data not shown).

It is widely accepted that the decomposition of organic peroxides is via the breaking of the weak O–O single bond. Scheme 2 displays the formation of alkoxycarboxyl free radicals $C_2H_5–O–CO_2^{\bullet}$ from primary dissociation of DEPDC.

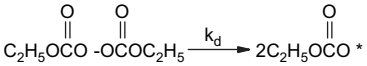

Scheme 2. Primary dissociation of DEPDC to form alkoxycarboxyl free radicals.

If the reaction of DEPDC decomposition is first-order

$$\frac{dC}{dt} = -k_d C \tag{2}$$

By integrating Eq. (2), and taking advantage of the linear relationship:

$$\frac{C_0}{C} = \frac{A_0}{A} \tag{3}$$

the following equation can be obtained:

$$\ln\frac{A_0}{A} = k_d t \tag{4}$$

From Eq. (4), the decomposition rate constant k_d can be determined with the experimental data absorbance A and time t. The absorbance intensities of the characteristic peaks at 1203 cm^{-1} in $scCO_2$ and at 1194 cm^{-1} in heptane were selected for kinetic study because these peaks effectively reflected the concentration of DEPDC, provided the best signal/noise ratio, and gave no observable superposition in this spectral region.

With the experimental data (A_0, A, t), a plot of $\ln(A_0/A)$ versus t can be obtained. Fig. 6 displays a typical plot of $\ln(A_0/A)$ versus time for DEPDC decomposition in heptane at 50 °C using the intensity of the characteristic peak at 1194 cm^{-1}. The linear plot of $\ln(A_0/A)$ versus time is strongly in agreement with the assumed first-order unimolecular decomposition mechanism, giving the decomposition rate constant, k_d, as the slope. In order to make a comparison with the previous studies reported for DEPDC decomposition, a study was conducted on a series of experiments of DEPDC decomposition in heptane under atmospheric N_2 at various temperatures between 40 and 74 °C. By means of plotting $\ln(A_0/A)$ versus t, the rate constants at different temperatures were obtained, as

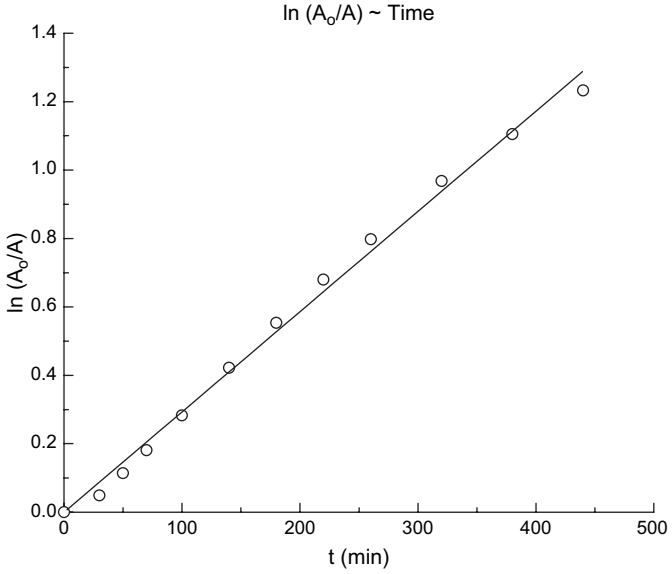

Fig. 6. Kinetic measurement of DEPDC thermal decomposition in heptane at 50 °C.

listed in Table 1. In light of the Arrhenius equation, $\ln k_d = \ln A_d - E_a/(RT)$, a plot of $\ln k_d$ versus $1/(RT)$ will give the activation energy as the absolute value of the slope. The plot of $\ln k_d$ versus $1/(RT)$ for DEPDC decomposition in heptane and $scCO_2$ is shown in Fig. 7. The activation energy (E_a) and pre-exponential factor (A_d) for thermal decomposition of DEPDC in heptane, determined from the plot with linear correlation coefficient being 0.992, are $E_a = 115$ kJ/mol and $A_d = 2.01 \times 10^{14}\ s^{-1}$. The 95% confidence limits of E_a and A_d are 95–135 kJ/mol and 1.36×10^{11}–$2.97 \times 10^{17}\ s^{-1}$, respectively.

For the decomposition of DEPDC in $scCO_2$, the linear $\ln(A_0/A)$–t plots in the temperature range from 40 to 60 °C indicate that the decomposition of DEPDC under supercritical conditions also occurred via first-order kinetics of unimolecular decomposition. The rate constants at different temperatures in $scCO_2$ are listed in Table 2. The activation energy (E_a) and pre-exponential factor (A_d) for decomposition of DEPDC in $scCO_2$, determined from the plot with linear correlation coefficient being 0.998, are $E_a = 118$ kJ/mol and $A_d = 4.54 \times 10^{14}\ s^{-1}$. The 95% confidence limits of E_a and A_d are 106–130 kJ/mol and 4.66×10^{12}–$4.42 \times 10^{16}\ s^{-1}$, respectively. However, as discussed further below, if the concentration of DEPDC became high enough in pure $scCO_2$, non-first-order kinetics and a different reaction mechanism were found.

Table 1
Decomposition rate of DEPDC in heptane under N_2

T (°C)	k_d (s^{-1})
40	7.8×10^{-6}
45	2.9×10^{-5}
50	4.8×10^{-5}
60	1.8×10^{-4}
70	5.2×10^{-4}
74	7.4×10^{-4}

$E_a = 115$ kJ/mol.

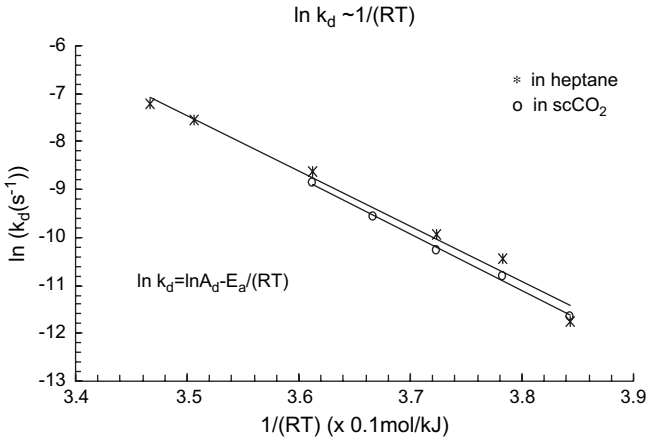

Fig. 7. Arrhenius plot of $\ln k_d$ versus $1/(RT)$ for DEPDC decomposition in $scCO_2$ and heptane.

As reported by Yamada *et al.* [16], the activation energy for the decomposition of dialkyl peroxydicarbonates is between 113 and 126 kJ/mol and tends to decrease with increasing alkyl group chain length. Our present results obtained by *in situ* FT-IR are in good agreement with the results obtained by the conventional titration method [16]. However, it still looks surprising that the rate constants and the activation energy data of the decomposition of DEPDC in the two solvents are similar. This can be explained by comparing the effects of viscosity and dielectric constants for the two solvents. On the one hand, the rate constant of decomposition of organic peroxides may be increased by lowering the viscosity of the solvent. It was reported that the decomposition rate constant increased as the solvent viscosity decreased for the thermal decomposition of a series of fluorinated diacyl peroxides in $scCO_2$ [30]. On the other hand, the rate constant of decomposition of initiators may be decreased by lowering the dielectric constant of solvents [29]. A dipolar interaction between the initiator's transition state and the solvent medium exists but radical reactions are not very solvent sensitive with rates that usually span less than an order of magnitude [35]. Hence, our similar kinetic results may be explained as $scCO_2$ has both a lower viscosity and a smaller dielectric constant than heptane.

The decomposition of DEPDC in $scCO_2$ was previously studied by Charpentier *et al.* [31] using a CSTR in the presence of galvinoxyl as a radical scavenger in the temperature range of 65–85 °C, wherein it was found that the decomposition of the DEPDC was first order and the reaction of an initiator radical with the radical scavenger is essentially instantaneous. The activation energy (E_a) and pre-exponential factor (A_d) for the decomposition of DEPDC in $scCO_2$ were determined as $E_a = 132 \pm 8$ kJ/mol and $A_d = (6.3 \pm 1.4) \times 10^{16}$ s^{-1}. This higher E_a found using the radical scavenger technique may be due to not all the free radicals from the decomposition reacting with the radical scavenger galvinoxyl. The reactions of radicals are complex and a small number of free radicals could be consumed in a variety of other ways without reacting with the scavenger to form the UV-detectable adduct.

Table 2
Decomposition rate of DEPDC in $scCO_2$

T (°C)	P (MPa)	k_d (s^{-1})
40	10.5	8.7×10^{-6}
45	12.1	2.0×10^{-5}
50	13.7	3.4×10^{-5}
55	15.2	7.0×10^{-5}
60	16.8	1.4×10^{-4}

CO_2 density = 15 mol/l. $E_a = 118$ kJ/mol.

Table 3
Comparison of k_d of thermal decomposition of DEPDC

Conditions (MPa)	Temperature (°C)	k_d (s^{-1})
$P_{N_2} = 0.07$	60	1.8×10^{-4}
$P_{CO_2} = 20.7$	60	6.0×10^{-5}
$P_{ethylene} = 13.8$	60	5.0×10^{-5}
$P_{ethylene}/P_{CO_2} = 6.9/13.8$	60	6.2×10^{-5}

The rate constants of DEPDC decomposition in both supercritical ethylene and supercritical ethylene/$scCO_2$ were measured and compiled in Table 3. It is seen that the decomposition rates of DEPDC under $scCO_2$ and supercritical ethylene are similar to one another, which implies that radical-induced decomposition is negligible for this system. Fig. 8 demonstrates the rate constants of DEPDC decomposition obtained from this study and from the literature using various other techniques. This figure suggests very strongly that the nature of the solvent has no significant effect on the rate constant for this initiator. Hence, high-pressure *in situ* FT-IR is very useful for studying the kinetics of initiator decomposition in supercritical fluids.

3.4. Decomposition mechanism of DEPDC in $scCO_2$

As described above, the thermal decomposition of low-concentration DEPDC in either $scCO_2$ or heptane is via first-order kinetics of unimolecular decomposition. In both solvent

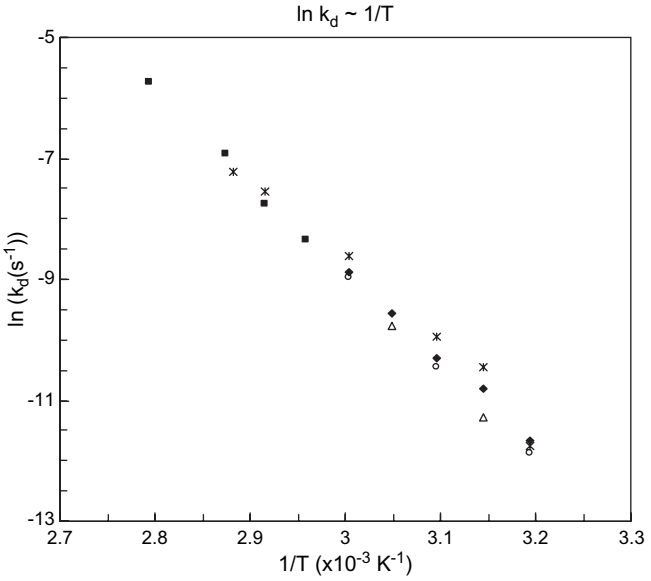

Fig. 8. Comparison of rate constants for diethyl peroxydicarbonate decomposition in $scCO_2$ (◆) and heptane (*), to those reported in the literature for the solvents such as $scCO_2$ (■), *tert*-butanol (△), and 2,2′-oxydiethylene bis(allyl carbonate) (○).

systems studied, the FT-IR spectra of the decomposed products from DEPDC show peaks in the ranges of 1747–1756 cm^{-1} and 1250–1262 cm^{-1}, which are assigned to the stretching vibrations of the C=O and C–O functional groups, respectively. Partial decarboxylation of the initially formed $C_2H_5OCO_2^{\bullet}$ radicals into $C_2H_5O^{\bullet}$ radicals and CO_2 cannot be excluded from the experimental observation, but the observed growing peaks of the carboxyl group in the reaction products with reaction time (1747 and 1262 cm^{-1} in Fig. 2 and 1756 and 1250 cm^{-1} in Fig. 3) suggest that most of the initially formed $C_2H_5OCO_2^{\bullet}$ radicals were not decarboxylated at the relatively low temperatures under the studied experimental conditions. The free radical $C_2H_5OCO_2^{\bullet}$ is extremely reactive and able to abstract a hydrogen atom from an available source if no monomer is present to polymerize. The gradually developed absorbance peaks at 1756 and 1250 cm^{-1} during the decomposition under $scCO_2$ conditions are likely attributed to the formed molecule, monoethyl carbonate (C_2H_5–O–CO_2H).

The extent of the decarboxylation of the free radicals strongly depends on both the structures of the free radicals and the experimental conditions. Studies on the initiator structure showed for example that CF_3OCO_2•decarboxylated faster than FCO_2•[36] while carbonyloxy radicals with a tertiary α-carbon atom decarboxylated much faster than radicals with a primary α-carbon atom [24]. For photoinduced decomposition of peroxides using C_6H_5–C(O)O–OR (R = benzoyl or *tert*-butyl) and *tert*-butyl 9-methylfluorene-9-percarboxylate, decarboxylation of the benzoyloxy and 9-methylfluorenylcarbonyloxy radicals took place on the picosecond time scale [26,28]. The ultrafast decarboxylation of these carbonyloxy radicals was explained by the high excess energy available after photoexcitation of the parent peroxides, and/or a fast and direct dissociation via electronically excited states. On the contrary, the alkoxycarboxyl radicals from the thermal decomposition of dicyclohexyl peroxydicarbonate did not readily decarboxylate before entering into reactions with solvent or bimolecular disproportionation at 50 °C, although the decarboxylation of alkoxycarboxyl radicals formed from OO-*tert*-butyl O-cyclohexyl peroxycarbonate became significant in the 100–110 °C range [22]. Decarboxylation of these radicals was slow relative to competing bimolecular reactions due to a high activation energy, so could be increased by higher temperatures [22]. Similarly, according to Buback *et al.*'s photoexcitation study on 2-Me–C_6H_4–$CO_2^{\bullet}$, intramolecular hydrogen atom migration was faster than decarboxylation at thermal energies associated with ambient temperatures, while higher energies increased the rate of decarboxylation [24]. Hence, our results showing little decarboxylation for DEPDC in $scCO_2$ and hexane is expected at the relatively low temperatures studied from 40 to 74 °C, and for the ethoxycarboxyl radical with a primary α-carbon atom.

To further probe the mechanism of decomposition of DEPDC in $scCO_2$, the reactor was first cooled down to ambient temperature and then the venting was carefully carried out to atmospheric pressure during a period of approximately 30 min. Fig. 9 exhibits the spectrum of the decomposition products observed at the bottom of the reactor after the thermal decomposition of DEPDC in $scCO_2$ and subsequent venting. The two previously developed broad peaks at 1756 and 1250 cm^{-1} are no longer dominant. Instead, the newly formed

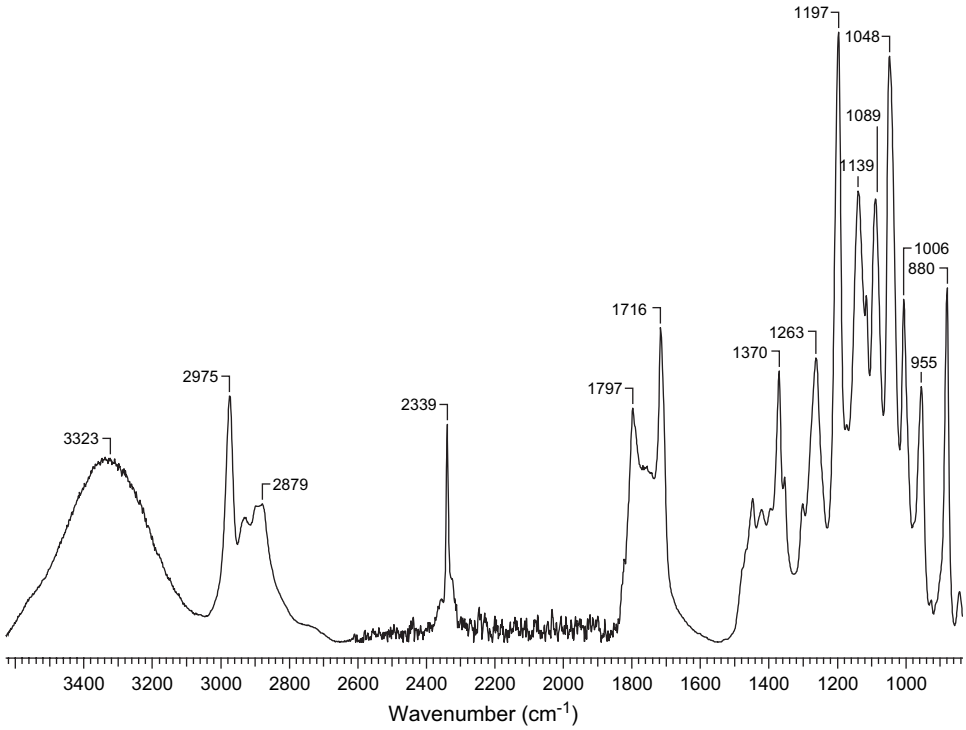

Fig. 9. FT-IR spectrum of thermal decomposition products after 860 min reaction in $scCO_2$ at 50 °C and 20 MPa then venting to atmospheric pressure. Spectra were collected at ambient temperature under atmospheric pressure.

peaks at 3323, 2975, 2879, 2339, 1797, 1716, 1370, 1263, 1197, 1089, 1048 and 880 cm^{-1} suggest the presence of new reaction products from decomposition. By referring to the literature and offline FT-IR experimental measurements, the peaks at 3323, 2975, 2879, 1089, 1048, and 880 cm^{-1} are attributed to ethanol, which was formed from the decarboxylation of the unstable intermediate giving rise to the peaks at 1756 and 1250 cm^{-1} when CO_2 was vented from the reactor. The peak at 1716 cm^{-1} in Fig. 9 can be assigned to 2,3-butanedione [37] while the peak at 2339 cm^{-1} indicates the existence of residual CO_2 and/or CO_2 from the conversion of residual monoethyl carbonate. It was unavoidable to lose some volatile decomposition products during the venting process, but the major end products would remain in the reaction residue at the bottom of the reactor. This reaction residue was further analyzed using NMR (^1H, ^{13}C, gCOSY, and gHSQC) [38], and the products ethanol, ethyl acetate, and 2,3-butanedione were found (see supplementary data).

Fig. 10a displays the spectrum of the high-purity DEPDC (without organic solvents) in a relatively high concentration in $scCO_2$. Heating this solution led to Fig. 10b, which displays the IR spectrum of the induced decomposition of the initiator. This decomposition reaction was completed within a few seconds with subsequent increase in temperature and pressure. Fig. 10b shows new peaks at 3424, 2980, 2887, 1727, 1096, and 1044 cm^{-1}. The peak at 1727 cm^{-1} can be assigned to acetaldehyde while the other five peaks are ascribed to ethanol, using the literature values [37–39]. Gas chromatography–mass spectrometry (GC–MS) was also utilized to study the DEPDC decomposition using the injection port as a microreactor according to a standard analysis technique by ASTM [40].

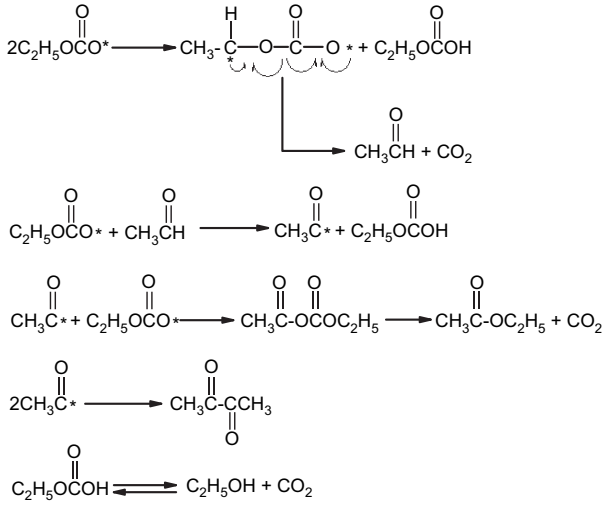

Scheme 3. Proposed mechanism of forming monoethyl carbonate, ethanol, ethyl acetate, and 2,3-butanedione in $scCO_2$.

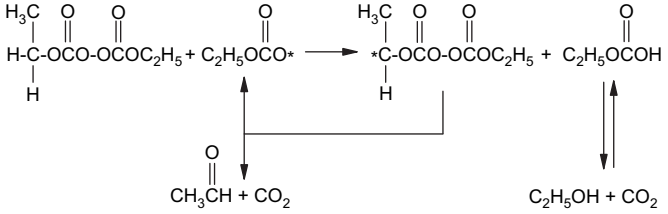

Scheme 4. Proposed mechanism of forming ethanol and acetaldehyde for the induced decomposition of DEPDC in $scCO_2$.

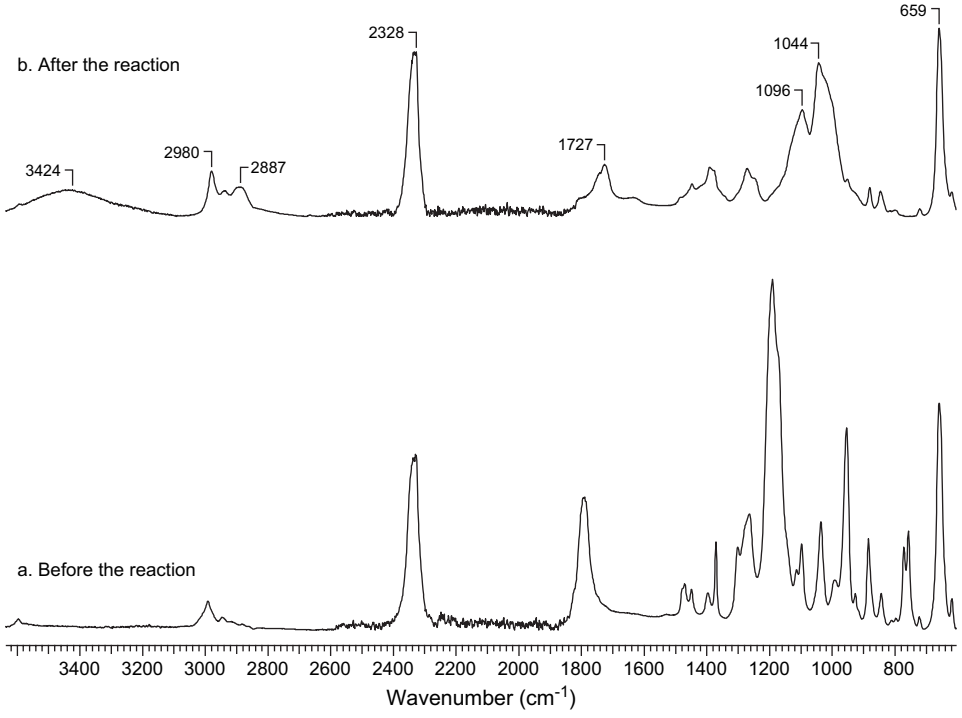

Fig. 10. *In situ* FT-IR spectra of DEPDC before and after the induced explosive decomposition in $scCO_2$ at 60 °C and 20 MPa (DEPDC concentration 18.4 wt%).

Table 4
Assignment of characteristic FT-IR peaks used in the study [33,37,39]

Chemicals	Frequency (cm^{-1})	Assignment
Heptane	2960–2850	CH_3 and CH_2 asym. and sym. stretching vibrations
	1467	CH_3 asym. bending/CH_2 scissoring vibrations
	1378	CH_3 sym. bending vibration (umbrella mode)
Diethyl peroxydicarbonate (DEPDC)	1794–1803	C=O stretching vibrations
	1191–1203	C–O stretching vibrations
Diethyl carbonate	1744–1751	C=O stretching vibrations
	1251–1262	O–C–O stretching vibrations
Decomposed products	1747	C=O stretching vibrations (in heptane)
	1756	C=O stretching vibrations (in $scCO_2$)
	1262	O–C–O stretching vibrations (in heptane)
	1250	O–C–O stretching vibrations (in $scCO_2$)
	3323–3424	O–H stretching vibrations (CH_3CH_2OH)
	2975–2980	CH_3 asym. stretching vibrations (CH_3CH_2OH)
	2879–2887	CH_2 asym. stretching vibrations (CH_3CH_2OH)
	1044–1048 and 1089–1096	C–O stretching vibrations (CH_3CH_2OH)
	1727	C=O stretching vibration (CH_3CHO)
	1716	C=O stretching vibration (2,3-butanedione)

MS fitting results similarly showed the presence of ethanol, ethyl acetate and butanediol (see supplementary data). These results are also in good agreement with the previous studies by Duynstee *et al.* [23] who found the major products from decomposition of a similar initiator, diisopropyl peroxydicarbonate, were isopropanol, acetone and CO_2, and Van Sickle [22] who found the major products from decomposition of dicyclohexyl peroxydicarbonate were CO_2, cyclohexanol, and cyclohexanone. Schemes 3 and 4 summarize the likely decomposition reactions under these experimental conditions. Assignments of these absorbance peaks of DEPDC, heptane, diethyl carbonate, ethanol, and other decomposed products are given in Table 4 as reference. It should be mentioned that in addition to the major products discussed above, other byproducts could also be produced in small amount due to the high reactivity of the free radicals. As the free-radical mechanisms are complex, these schemes should be taken as descriptive.

4. Conclusions

This study has shown the great advantage of using *in situ* ATR-FT-IR in studying the mechanism and kinetics of the thermal decomposition of diethyl peroxydicarbonate (DEPDC) in supercritical fluids (under high pressure). Two new characteristic peaks, appeared at 1747–1756 and 1250–1262 cm^{-1} simultaneously with the decomposition of DEPDC, demonstrate that the major decomposed products contain a carboxyl group and decarboxylation of the initially formed $ROCO_2^{\bullet}$ radicals does not occur significantly. By comparison with standard IR spectra, the two peaks are assigned to the formation of carbonates from the decomposition of DEPDC. For DEPDC decomposition in supercritical CO_2, the first formed intermediate monoethyl carbonate was decarboxylated and converted into ethanol during removal of CO_2. Through the kinetic measurements, the decomposition of DEPDC is revealed as in the first-order kinetics of unimolecular reaction regardless of the applied media. The activation energy of the thermal decomposition of DEPDC was obtained to be 115 kJ/mol in heptane from 40 to 74 °C and 118 kJ/mol in $scCO_2$ from 40 to 60 °C.

Acknowledgements

This work was financially supported by the Canadian Natural Science and Engineering Research Council (NSERC), the Ontario Centres of Excellence (OCE), the Canadian Foundation for Innovation (CFI), the Ontario Premiers Research Excellence Award (PREA). Special thanks go to Dr. Alex Henderson and Dr. Warren Baker at AT Plastics for fruitful discussions.

Appendix A. Supplementary data

Supplementary data associated with this article can be found in the online version, at doi:10.1016/j.polymer.2006.12.018.

References

[1] DeSimone JM, Tumas W. Green chemistry using liquid and supercritical carbon dioxide. New York, NY: Oxford University Press, Inc.; 2003.
[2] DeSimone JM, Guan Z, Elsbernd CS. Science 1992;257:945.
[3] Kendall JL, Canelas DA, Young JL, DeSimone JM. Chem Rev 1999; 99(2):543.
[4] Charpentier PA, DeSimone JM, Roberts GW. ACS Symp Ser 2002;819: 113.
[5] Charpentier PA, DeSimone JM, Roberts GW. Ind Eng Chem Res 2000; 39:4588.
[6] Maartje K, Tjerk V, Marius V, Jos K. Chem Eng Sci 2001;56(13):4197.
[7] Johnston KP, Shah PS. Science 2004;303:482.
[8] Sui R, Rizkalla AS, Charpentier PA. Langmuir 2005;21(14):6150.
[9] McHugh MA, Krukonis VJ. Supercritical fluid extraction: principles and practice. Boston: Butterworth-Heinemann; 1994.
[10] DeSimone JM, Maury EE, Lemert RM, Combes JR. Makromol Chem Macromol Symp 1993;67:251.
[11] Chem Week 2002;164(13):24.
[12] Gill GB. Synthetic use of free radicals. In: Modern reactions in organic synthesis. London: Van Nostrand Reinhold Company LTD; 1970.

[13] Cohen SG, Sparrow DB. J Am Chem Soc 1950;72:611.
[14] Oldfield FF, Yasuda HK. J Biomed Mater Res 1999;44:436.
[15] Spantulescu MD, Jain RP, Derksen DJ, Vederas JC. Org Lett 2003;5: 2963.
[16] Yamada M, Kitagawa K, Komai T. Plast Ind News 1971;17(9):131.
[17] Beristain MF, Bucio E, Burillo G, Muñoz E, Ogawa T. Polym Bull 1999; 43(4/5):357.
[18] Pérez C, Cassano G, Vallés E, Failla M, Quinzani L. Polymer 2002;43: 2711.
[19] Danilov A, Mitusova T, Kovalev V, Churzin A. Chem Technol Fuels Oils 2003;39:330.
[20] Hara Y, Notomi Y, Nakamura H, Shimizu M, Jinnouchi T. J Ind Explosives Soc Jpn 1992;53:254.
[21] O'Driscoll KF. Organic peroxides in vinyl polymerization. In: Organic peroxides. New York: Wiley-Interscience; 1970.
[22] Van Sickle DE. J Org Chem 1969;34(11):3446.
[23] Duynstee EFJ, Esser ML, Schellekens R. Eur Polym J 1980;16(12):1127.
[24] Buback M, Kling M, Schmatz S, Schroeder J. Phys Chem Chem Phys 2004;6(24):5441.
[25] Abel B, Assmann J, Botschwina P, Buback M, Kling M, Oswald R, et al. J Phys Chem A 2003;107(26):5157.
[26] Abel B, Buback M, Kling M, Schmatz S, Schroeder J. J Am Chem Soc 2003;125(43):13274.
[27] Abel B, Assmann J, Buback M, Grimm C, Kling M, Schmatz S, et al. J Phys Chem A 2003;107(45):9499.
[28] Aschenbrucker J, Buback M, Ernsting NP, Schroeder J, Steegmuller U. J Phys Chem B 1998;102(29):5552.
[29] Guan Z, Combes JR, Menceloglu YZ, DeSimone JM. Macromolecules 1993;26:2663.
[30] Bunyard WC, Kadla JF, DeSimone JM. J Am Chem Soc 2001;123(30): 7199.
[31] Charpentier PA, DeSimone JM, Roberts GW. Chem Eng Sci 2000;55: 5341.
[32] Kadla JF, DeYoung JP, DeSimone JM. Polym Prepr 1998;39(2):835. Division of Polymer Chemistry, ACS.
[33] Socrates G. Infrared and Raman characteristic group frequencies: tables and charts. Chichester: John Wiley & Sons Ltd; 2001.
[34] Vacque V, Sombret B, Huvenne J, Legrand P, Suc S. Spectrachim Acta A Mol Biomol Spectrosc 1997;53:55.
[35] Reichardt C. Solvents and solvent effects in organic chemistry. Weinheim: VCH; 1988.
[36] Burgos Paci MA, Arguello GA, Garcia P, Willner H. J Phys Chem A 2005;109(33):7481.
[37] Pavia DL, Lampman GM, Kriz GS. Introduction to spectroscopy. Orlando: Harcourt, Inc.; 2001.
[38] From Sigma–Aldrich websites, standard ^{1}H, ^{13}C NMR spectra of ethyl acetate, 2,3-butanedione, diethyl carbonate, acetaldehyde, and ethanol were used and compared with the spectra from DEPDC decomposition in present study.
[39] From NIST websites, standard IR spectra of ethyl acetate, 2,3-butanedione, diethyl carbonate, dimethyl carbonate, acetic acid, acetaldehyde, and ethanol were used and compared with the spectra from DEPDC decomposition in present study.
[40] ASTM, E475-95.